iScience

Article

α- and β-myosin II can be non-uniformly distributed within the cardiac sarcomere

Graphical abstract

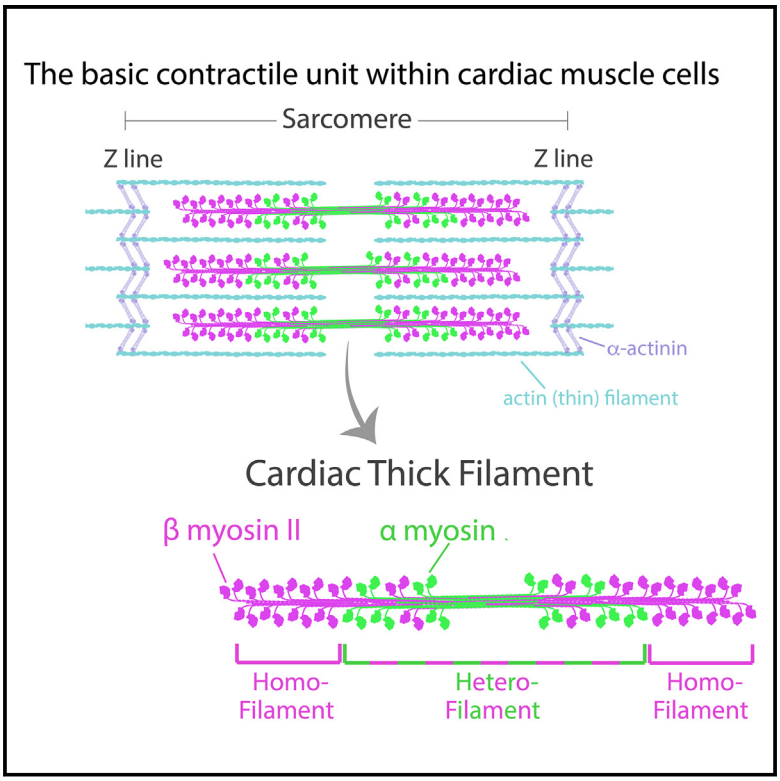

Highlights

- α- and β-myosin II can exhibit a non-uniform distribution within the cardiac sarcomere
- α-myosin II motors can localize primarily to a central region of cardiac thick filament stacks
- β-myosin II motors extend throughout cardiac thick filament stacks
- Myosin isoform distribution may regulate the mechanical properties of thick filaments

Authors

James B. Hayes, Alaina H. Willet, Leah R. Caplan, Ela W. Knapik, Matthew J. Tyska, Dylan T. Burnette

Correspondence

dylan.burnette@vanderbilt.edu

In brief

Cardiovascular medicine; Cell biology

Hayes et al., 2025, iScience *28*, 112233
April 18, 2025
https://doi.org/10.1016/j.isci.2025.112233

CellPress

iScience

CellPress
OPEN ACCESS

Article

α- and β-myosin II can be non-uniformly distributed within the cardiac sarcomere

James B. Hayes,[1] Alaina H. Willet,[1] Leah R. Caplan,[1] Ela W. Knapik,[1,2] Matthew J. Tyska,[1] and Dylan T. Burnette[1,3,*]
[1]Department of Cell and Developmental Biology, Vanderbilt University School of Medicine Basic Sciences, Nashville, TN, USA
[2]Division of Genetic Medicine, Department of Medicine, Vanderbilt University Medical Center, Nashville, TN, USA
[3]Lead contact
*Correspondence: dylan.burnette@vanderbilt.edu
https://doi.org/10.1016/j.isci.2025.112233

SUMMARY

In humans, the forces of the heartbeat are generated by both "fast" α-myosin II and "slow" β-myosin II molecular motors. Here, we report that α-myosin II and β-myosin II can take on an anisotropic arrangement within cardiac sarcomeres, the minimal contractile unit of cardiac muscle. In induced pluripotent stem cell (iPSC)-derived cardiac myocytes, we find that α-myosin II is distributed primarily within the central region of the filaments, being mostly absent from the distal ends, whereas β-myosin II is distributed along the entire filament. We measure that the outer bounds of α-myosin II in filament stacks are shorter than those of β-myosin II in both the zebrafish embryo and adult human myocardium. Our findings suggest that the two motors that drive the human heartbeat can have a specific and non-uniform arrangement within cardiac thick filaments, which may be thus divided into two distinct mechanical regions based on myosin II motor composition. We suggest potential roles for each motor during contraction-relaxation based on these distributions and recent literature.

INTRODUCTION

Cardiac sarcomeres are the minimal unit of cardiac muscle contraction and drive the heartbeat.[1] Sarcomeres contain thick filaments comprising the molecular motor myosin II.[2] The classical arrangement of myosin II molecules in thick filaments is a bipolar array, with the tails of the molecules facing the filament center and the motor domains extending outward. Electron micrographs have demonstrated that thick filaments in striated muscle have a typical length within a sarcomere, and recent high-resolution electron microscopy reconstructions of cardiac thick filaments have revealed the relative positioning of individual myosin II motors within filaments.[3–5]

Recent studies have suggested that the spatial position of myosin II motors along the filament long-axis influences what role they play in muscle contraction.[4–8] In humans, cardiac contractions are driven by two different types of myosin II motor, α-myosin II and β-myosin II.[9] α- and β-myosin II motors are sufficiently similar in structure as to be indistinguishable by electron microscopy, and mutation or loss of either is associated with heart failure.[10–12] For these reasons, it is of great interest to determine how they are spatially arranged within filaments.

RESULTS

Non-uniform distribution of α- and β-myosin II in human iPSC-derived cardiac myocytes

In cardiac myocytes (heart muscle cells), stacks of myosin II filaments form the core of each sarcomere. We used human induced pluripotent stem cell (iPSC)-derived cardiac myocytes (hiCMs) in combination with super-resolution imaging to determine if we could simultaneously localize α-myosin II and β-myosin II within these filament stacks. We first exogenously expressed mEGFP-*MYH6*, which encodes fluorescent mEGFP attached to the motor domain—N terminus—of α-myosin II. We then fixed and stained mEGFP-*MYH6*-expressing hiCMs with antibodies raised against the motor domain of β-myosin II. Representative fluorescence images are shown in Figure 1A. β-myosin II stains appeared to follow the expected pattern of myosin II motors within a thick filament: a bipolar array of ∼1.4 μm length centered around a motorless "bare zone" (Figure 1A, top). In contrast, despite also being in bipolar arrays, α-myosin II motors appeared to be concentrated within a central ∼1.0 μm region of filaments (Figure 1A, middle).

To directly compare the distributions of α- and β-myosin II within filaments, we drew line scans across multiple filament stacks and plotted the resulting fluorescence distributions using the image analysis tool Fiji. The resulting curves suggested that in individual filament stacks, α- and β-myosin II motors are centered around the same bare zone, but β-myosin II motors extend further outward than α-myosin II motors (Figure 1B). To determine the consistency of the distribution, we centered line scans within the bare zones of individual filament stacks, plotted the resulting fluorescence distributions, and compiled the distributions of multiple line scans across multiple cells. The population-averaged distributions across three separate experiments suggest that α-myosin II motors are generally concentrated within the center of filaments, while β-myosin II motors extend further outward (Figure 1C).

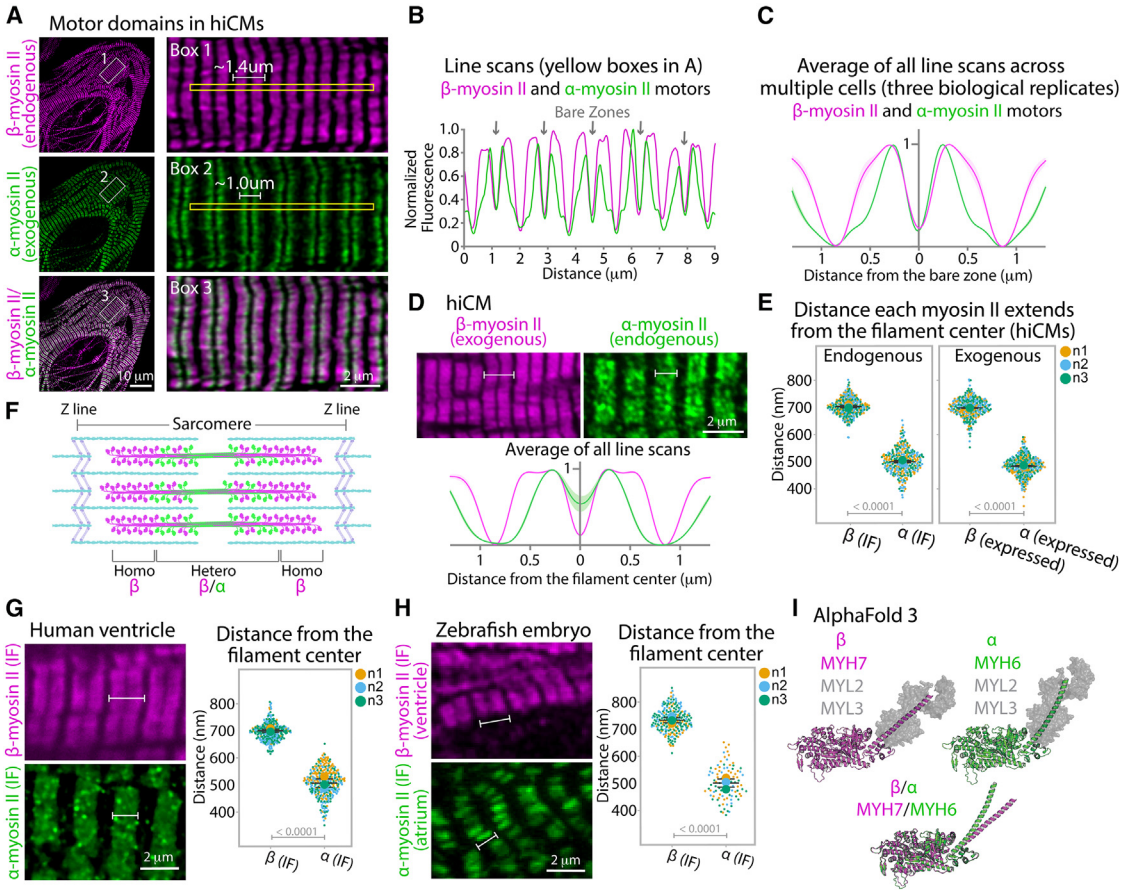

Figure 1. α- and β-myosin II can exhibit unique distributions within cardiac sarcomeres

(A) Representative example of IF of endogenous β-myosin II (top) and expression of mEGFP-*MYH6* (middle) in a hiCM; bottom shows overlay. Scale bars: left 10 μm, right 2 μm.

(B) Line scan from yellow boxes in (A).

(C) Average of all line scans (20 cells, 772 sarcomeres, 3 independent experiments). Lines show population-averaged mean value while shaded bands show ± standard error of the mean.

(D) Top: expression of mNeon-*MYH7* and IF of endogenous α-myosin II in a representative hiCM. Bottom: Average of all line scans (15 cells, 456 sarcomeres, 3 independent experiments). Lines show population-averaged mean value while shaded bands show ± standard error of the mean. White brackets denote individual filament stacks. Scale bar: 2 μm.

(E) Distance each myosin II extended from filament center in hiCMs (β-myosin II IF: 14 cells, 280 measurements; α-myosin II IF: 15 cells, 300 measurements; mNeon-*MYH7* (β expressed): 15 cells, 300 measurements; mEGFP-*MYH6* (α expressed): 15 cells, 300 measurements). *p*-values in grey (Welch's t-test).

(F) Simplified model of the potential arrangement of β-myosin II (magenta) and α-myosin II (green) in thick filaments of iPSC-derived cardiac myocyte sarcomeres.

(G) Left: IF using antibodies against β-myosin II (top) and α-myosin II (bottom) in different sections of human ventricle; right: distance the fluorescent signal of each myosin extended from the filament center (β-myosin II: 280 measurements; α-myosin II: 321 measurements). Scale bar: 2 μm. *p*-values in grey (Welch's t-test).

(H) Left: individual β-myosin II (ventricle) and α-myosin II (atrium) whole-mount immunofluorescence stains in 72 h post-fertilization zebrafish embryos; right: distance the fluorescent signal of each myosin extended from the filament center (β-myosin II: 14 embryos, 222 measurements; α-myosin II: 13 embryos, 102 measurements). White brackets in each image denote individual filament stacks. Scale bar: 2 μm. *p*-values in grey (Welch's t-test);

(I) AlphaFold3-predicted model of α-myosin II/β-myosin II heavy chain (*MYH6*/*MYH7* genes, respectively) motors + motor/lever arms, modeled with *MYL2*/*MYL3* (gray), which encode the ventricular essential/regulatory myosin light chains (a similar AlphaFold3-predicted model, but modeled with atrial essential/regulatory myosin light chains instead of ventricular light chains, is shown in supplement information).

N1, 2, and 3 in (E), (G), and (H) represent individual biological replicates, color-coded by replicate.

Next, we performed a reciprocal experiment, whereby we exogenously expressed mNeon-*MYH7* (which encodes fluorescent mNeon attached to the motor domain of β-myosin II), then fixed and stained mNeon-*MYH7*-expressing hiCMs with antibodies raised against α-myosin II. The resulting distribution patterns of exogenous β-myosin II and endogenous α-myosin II resembled those of exogenous α-myosin II and endogenous β-myosin II (Figures 1D and S1A). Taken together with Figures 1A–1C, these data suggest that β-myosin II and α-myosin II exhibit a consistent and non-uniform distribution within the sarcomeres of iPSC-derived cardiac myocytes.

To determine the distance that α- and β-myosin II extended from the filament center in hiCMs, we measured the length that the endogenous form of each extended from the bare zone using immunofluorescence (IF). Across multiple cells and experiments, the fluorescence signal from β-myosin II stains extended, on average, 702 nm from the center (on each side), while the signal from α-myosin II stains extended 499 nm (Figure 1E, left). To confirm these results, we next measured the length that exogenously expressed forms of each myosin II extended from the bare zone. Across multiple cells and experiments, the fluorescence signal from the exogenously expressed mNeon-*MYH7* fusion (β-myosin II) extended 698 nm while the signal from the mEGFP-*MYH6* fusion (α-myosin II) extended 483 nm (Figure 1E, right). We also measured the fluorescence signal of another α-myosin II fusion, mEOS-*MYH6*, which extended 535 nm (Figure S1B). In filaments with both motors, these data suggest most or all α-myosin II would be concentrated within a central ~500 nm of each half-filament, while the remainder would be mostly or all β-myosin II. Taking data from Figures 1A–1E together, we conclude that each cardiac myosin II has a unique spatial distribution within thick filaments of hiCMs, as depicted in the cartoon in Figure 1F.

Conserved myosin II distribution in human and zebrafish cardiac muscle

Recent electron microscopy-based reconstructions were generated from sections of adult ventricular tissue,[5] and a classic study reported that ~50% of ventricular myocytes stained positive for both α- and β-myosin II.[10] Therefore, we next localized α- and β-myosin II via IF in sections of ventricular muscle from human adults and measured the length that each extended from the filament center. Similar to hiCMs, the fluorescent signal from β-myosin II stains in human tissue extended 696 nm outward from the center while signal from α-myosin II stains extended 510 nm (Figures 1G and S1C). We next asked if each myosin II would make a filament of unique length in the apparent absence of the other. To test this, we localized each myosin using IF in the developing zebrafish embryo, where expression of the zebrafish β-myosin II ortholog is restricted to the ventricle while the α-myosin II ortholog is restricted to the atrium.[13] The fluorescence signal from β-myosin II stains (in the embryonic ventricle) extended 734 nm from the filament center while fluorescence signal from α-myosin II stains (in the embryonic atrium) extended 507 nm (Figures 1H and S1D), each matching measurements of each myosin in the human ventricle. These data suggest that the outer bounds of α- and β-myosin II within cardiac thick filaments are evolutionarily conserved and are not dependent on the presence of the other myosin II.

DISCUSSION

Answering what limits the outer bounds of each myosin II within a filament will require a combination of complex methodologies, spanning cellular, protein, and structural biology. The amino acid sequences of the proteins which contain, respectively, the α-myosin II motor (encoded by *MYH6*) and the β-myosin II motor (encoded by *MYH7*) are 93% similar, but regions of sequence divergence are nonetheless predicted to produce structural differences. For example, sequence divergence in the lever arm (Figure S1E) is predicted to result in unique motor-lever arm angles for α- vs. β-myosin II (Figures 1I and S1F). Structural differences such as these, post-translational modifications, or interactions with other proteins might each individually, or in some combination, contribute to the resulting differences in distributions of the two myosins.

Our data do not preclude the possibility that α-myosin II could in some contexts populate the entire length of thick filaments. For instance, in myocardium where α-myosin II is predominantly expressed (such as the adult human atrium), the distribution of α-myosin II within filaments may differ from our findings. Nonetheless, in light of our results, it is of interest to consider how a thick filament containing a central mixture of α- and β-myosin II motors, flanked by distal regions of all or mostly β-myosin II motors, fits within current paradigms of muscle contraction-relaxation. During contraction, X-ray diffraction experiments have suggested that distal motors are activated first and that central motors bear the peak forces.[6] Our data suggest that distal motors can, at least in certain contexts, be all or mostly β-myosin II motors, while central motors might be more likely to contain a mixture of both α- and β-myosin II motors. Within the central region of filaments, "fast" α-myosin II motors may actively contribute to peak force or regulate it by rapidly generating tension along the filament backbone, activating additional motors according to the thick filament mechano-sensing hypothesis.[14] Fast α-myosin II motors within this region may also serve to locally increase thin filament sensitivity to calcium, promoting contractility by enhancing cooperative binding.[6] After reaching peak force, central α-myosin II motors may serve to promote relaxation by rapidly reducing strain experienced by distal filament motors in rigor, de-activating those motors.[6,14] Thus, the data we present here should be contextualized into models and paradigms of spatiotemporal kinetics, structure, and force generation of cardiac muscle. Finally, given the association of decreased α-myosin II with heart disease,[10–12] and our data suggesting that α-myosin II motors may be more concentrated where force generation is at a maximum, we postulate that α-myosin II-associated heart failure may be a direct consequence of a contractile defect originating within the central region of the thick filament.

Limitations of the study

This study utilized iPSC-derived cardiac myocytes that are mostly ventricular-like and are most akin to cardiac myocytes in the developmental state. Furthermore, human tissue sections were obtained only from ventricular tissue sections and not atrial sections. Therefore, the major caveats of this study are whether the reported non-uniform distributions of myosin II paralogs herein are specific to a developmental and/or are unique to cardiac myocytes of the ventricular heart chamber.

RESOURCE AVAILABILITY

Lead contact

Requests for further information and resources should be directed to and will be fulfilled by the lead contact, Dylan Burnette (dylan.burnette@vanderbilt.edu).

Materials availability

All plasmids used/generated in this study are available upon request.

Data and code availability

- All data used in this study are preserved in online database and are available upon request.
- No code was generated for this work.
- Any additional information required to reanalyze the data reported in this paper is available from the lead contact upon request.

ACKNOWLEDGMENTS

We would like to thank Kari Seedle at the Vanderbilt Nikon Center for Excellence and the Vanderbilt Center for Imaging Shared Resources (CISR) for experimental and imaging assistance. We also thank Yan Ru Su and the Vanderbilt Cardiology Core for graciously providing samples of normal human ventricular myocardium. Finally, we thank Cory Guthrie, Dharmendra Choudhary, and those at the Vanderbilt Zebrafish core for setting up crosses for zebrafish embryos. This work was supported by a grant from the National Institute of General Medical Sciences (R35 GM125028) to D.T.B. and a graduate student fellowship from the American Heart Association (836090) to J.B.H.

AUTHOR CONTRIBUTIONS

J.B.H. and D.T.B. conceived of the study, planned the experiments, and wrote the manuscript. J.B.H. performed all imaging, data analysis, and statistical testing. A.W. provided AlphaFold3-generated structures. J.B.H. performed zebrafish whole-mount stains. L.R.C. performed human tissue stains.

DECLARATION OF INTERESTS

The authors declare no competing interests.

STAR★METHODS

Detailed methods are provided in the online version of this paper and include the following:

- KEY RESOURCES TABLE
- EXPERIMENTAL MODEL AND STUDY PARTICIPANT DETAILS
  - Ethical approval
  - Zebrafish embryos
  - Cell culture
  - Human tissue samples
- METHOD DETAILS
  - hiCM transfection procedure
  - hiCM plating procedure
  - Immunofluorescence staining procedure
  - Human tissue stains
  - Zebrafish stains
  - Antibodies used in this study
  - Expression constructs
  - Imaging
- QUANTIFICATION AND STATISTICAL ANALYSIS

SUPPLEMENTAL INFORMATION

Supplemental information can be found online at https://doi.org/10.1016/j.isci.2025.112233.

Received: October 8, 2024
Revised: January 29, 2025
Accepted: March 13, 2025
Published: March 18, 2025

REFERENCES

1. Gordon, A.M., Homsher, E., and Regnier, M. (2000). Regulation of contraction in striated muscle. Physiol. Rev. *80*, 853–924. https://doi.org/10.1152/physrev.2000.80.2.853.

2. Tobacman, L.S. (1996). Thin filament-mediated regulation of cardiac contraction. Annu. Rev. Physiol. *58*, 447–481. https://doi.org/10.1146/annurev.ph.58.030196.002311.

3. Skubiszak, L., and Kowalczyk, L. (2002). Myosin molecule packing within the vertebrate skeletal muscle thick filaments. A complete bipolar model. Acta Biochim. Pol. *49*, 829–840.

4. Chen, L., Liu, J., Rastegarpouyani, H., Janssen, P.M.L., Pinto, J.R., and Taylor, K.A. (2024). Structure of mavacamten-free human cardiac thick filaments within the sarcomere by cryoelectron tomography. Proc. Natl. Acad. Sci. USA *121*, e2311883121. https://doi.org/10.1073/pnas.2311883121.

5. Dutta, D., Nguyen, V., Campbell, K.S., Padrón, R., and Craig, R. (2023). Cryo-EM structure of the human cardiac myosin filament. Nature *623*, 853–862. https://doi.org/10.1038/s41586-023-06691-4.

6. Brunello, E., Fusi, L., Ghisleni, A., Park-Holohan, S.J., Ovejero, J.G., Narayanan, T., and Irving, M. (2020). Myosin filament-based regulation of the dynamics of contraction in heart muscle. Proc. Natl. Acad. Sci. USA *117*, 8177–8186. https://doi.org/10.1073/pnas.1920632117.

7. Previs, M.J., Beck Previs, S., Gulick, J., Robbins, J., and Warshaw, D.M. (2012). Molecular mechanics of cardiac myosin-binding protein C in native thick filaments. Science *337*, 1215–1218. https://doi.org/10.1126/science.1223602.

8. Previs, M.J., Prosser, B.L., Mun, J.Y., Previs, S.B., Gulick, J., Lee, K., Robbins, J., Craig, R., Lederer, W.J., and Warshaw, D.M. (2015). Myosin-binding protein C corrects an intrinsic inhomogeneity in cardiac excitation-contraction coupling. Sci. Adv. *1*, e1400205. https://doi.org/10.1126/sciadv.1400205.

9. Walklate, J., Ferrantini, C., Johnson, C.A., Tesi, C., Poggesi, C., and Geeves, M.A. (2021). Alpha and beta myosin isoforms and human atrial and ventricular contraction. Cell. Mol. Life Sci. *78*, 7309–7337. https://doi.org/10.1007/s00018-021-03971-y.

10. Bouvagnet, P., Mairhofer, H., Leger, J.O., Puech, P., and Leger, J.J. (1989). Distribution pattern of alpha and beta myosin in normal and diseased human ventricular myocardium. Basic Res. Cardiol. *84*, 91–102. https://doi.org/10.1007/BF01907006.

11. Herron, T.J., and McDonald, K.S. (2002). Small amounts of alpha-myosin heavy chain isoform expression significantly increase power output of rat cardiac myocyte fragments. Circ. Res. *90*, 1150–1152. https://doi.org/10.1161/01.res.0000022879.57270.11.

12. Miyata, S., Minobe, W., Bristow, M.R., and Leinwand, L.A. (2000). Myosin heavy chain isoform expression in the failing and nonfailing human heart. Circ. Res. *86*, 386–390. https://doi.org/10.1161/01.res.86.4.386.

13. Yelon, D., Horne, S.A., and Stainier, D.Y. (1999). Restricted expression of cardiac myosin genes reveals regulated aspects of heart tube assembly in zebrafish. Dev. Biol. *214*, 23–37. https://doi.org/10.1006/dbio.1999.9406.

14. Linari, M., Brunello, E., Reconditi, M., Fusi, L., Caremani, M., Narayanan, T., Piazzesi, G., Lombardi, V., and Irving, M. (2015). Force generation by skeletal muscle is controlled by mechanosensing in myosin filaments. Nature *528*, 276–279. https://doi.org/10.1038/nature15727.

15. Schneider, C.A., Rasband, W.S., and Eliceiri, K.W. (2012). NIH Image to ImageJ: 25 years of image analysis. Nat. Methods *9*, 671–675. https://doi.org/10.1038/nmeth.2089.

16. Inoue, D., and Wittbrodt, J. (2011). One for all–a highly efficient and versatile method for fluorescent immunostaining in fish embryos. PLoS One *6*, e19713. https://doi.org/10.1371/journal.pone.0019713.

STAR★METHODS

KEY RESOURCES TABLE

REAGENT or RESOURCE	SOURCE	IDENTIFIER
Antibodies		
Alexa Fluor 647 goat anti-mouse IgG	Fisher Scientific	Cat# A-21235; RRID: AB_2535804
MYH7: myosin heavy chain mouse IgG	Developmental Studies Hybridoma Bank (DSHB)	Cat# A4.951; RRID: AB_528385
MYH6: atrium-specific myosin heavy chain mouse IgG	Developmental Studies Hybridoma Bank (DSHB)	Cat# S46; RRID: AB_528376
Biological samples		
Healthy adult human myocardial tissue (ventricle free wall)	Vanderbilt Cardiology Core (CLCTR)	16-013; 11-001; 12-007
Experimental models: Cell lines		
iCell Cardiomyocytes[2]	Fujifilm Cellular Dynamics	CMM-100-012-000.5
Experimental models: Organisms/strains		
Zebrafish *danio rerio* strain AB (wild-type)	IA-VUMC Zebrafish Aquatic Facility	RRID:ZFIN_ZDB-GENO-960809-7
Recombinant DNA		
Plasmid: mNeon-*MYH7*	This paper	N/A
Plasmid: mEGFP-*MYH6*	This paper	N/A
Plasmid: mEOS-*MYH6*	This paper	N/A
Software and algorithms		
ImageJ	Schneider et al.[15]	https://imagej.nih.gov/ij/

EXPERIMENTAL MODEL AND STUDY PARTICIPANT DETAILS

Ethical approval

All animal and human studies were done in accordance with NIH, the US Department of Agriculture Animal Welfare Act, and the US Public Health Service Policy on Humane Care and Use of Laboratory Animals and were approved by Vanderbilt University Medical Center's Institutional Animal Care and Use Committee. Zebrafish embryo experiments were conducted in accordance with M2100073-00-S2300172. Human tissue for staining was acquired from the Vanderbilt Cardiology Core under the approval of IRB# 240465.

Zebrafish embryos

Zebrafish (*danio rerio* wild-type strain AB) were raised under standard laboratory conditions at 28.5C with a constant photoperiod (14 h light, 10 h dark). Zebrafish embryos were kept in egg water at 28.5C until anesthetization in Tricaine and fixation at 72 h post-fertilization, which is before sex has been specified. Whole mount immunofluorescence stains were performed following fixation of zebrafish embryos at 4C overnight.

Cell culture

Human induced pluripotent stem cell-derived cardiac myocytes (hiCMs) were obtained from Fujifilm Cellular Dynamics (iCell Cardiomyocytes2; catalog # CMM-100-012-000.5) and cultured following the manufacturer's guidelines. In brief, the hiCMs were thawed and plated in 100uL per well Cardiomyocyte Plating Medium (Fujifilm Cellular Dynamics; catalog #R1151) at a density of 50,000 cells per well in 96-well polystyrene cell-culture plates pre-coated for 2 h with gelatin (EMD Millipore; catalog # ES-006-B). The Cardiomyocyte Plating Medium was replaced with pre-warmed iCell Cardiomyocytes Maintenance Medium (Fujifilm Cellular Dynamics; catalog #M1003) 5 h post-thawing, then again every 48 h. The cells were kept at 37°C with 5% CO2. All hiCMs used in this study were generated from fibroblast cells isolated from a healthy female from European descent. Cell line authentication is performed by Fujifilm Cellular Dynamics (FCDI) for each FDCI iPSC-derived cell line and involves the assignment of a 5-digit genomic DNA fingerprint ID for each tissue sample used for iSPC generation. 5-digit IDs for each iPSC-generated lot are provided with each purchased iPSC kit from FDCI.

Human tissue samples

Tissue sections were from human myocardial tissue isolated from the left ventricular free wall. Stains were performed using three separately isolated tissue sections: section 1 (ID 16-013) was isolated from a 62 years white female, section 2 (ID 11-001) was isolated from a 51 years Hispanic/latino male; section 3 (ID 12-007) was isolated from a 21 years white male.

METHOD DETAILS

hiCM transfection procedure

For experiments where exogenous expression of GFP-*MYH6*, mEOS-*MYH6,* or mNeon-*MYH7* was desired, hiCMs were transfected in 96-well plates 24 h prior to plating for immunofluorescence (for plating procedure, see below). To transfect myocytes, Promega ViaFect (cat# E498A) was combined with 100 ng plasmid DNA in Opti-MEM (Gibco; cat# 11058-021) at a ratio of 0.6 μL ViaFect:100 ng DNA for 45 min, then mixed into cardiomyocyte maintenance medium and applied to hiCMs for 18–24 h.

hiCM plating procedure

The plating procedure was as follows: hiCMs in 96-well plates were washed twice with 100 μL of 1X PBS without Ca2+ or Mg2+ (Gibco cat# 70011044), then trypsinized for 2.5 min with 40 μL of 0.1% Trypsin-EDTA without phenol red (Gibco cat# 15400054). Trypsin activity was halted by adding 120 μL of maintenance medium, and the cells were centrifuged at 0.2 rcf for 3 min. After centrifugation, the supernatant was removed, and the pellet was resuspended in maintenance medium. The resuspended cells were then pipetted onto 35 mm Cellvis cover glasses (10 mm; cat# D35-10-1.5-N) which had been coated with 10 μg/mL human fibronectin (Corning, cat# 354008) for 1 h prior to re-plating.

Immunofluorescence staining procedure

48 h after plating, 100uM s-nitro-blebbistatin (Sigma) was added to hiCMs in warm media for 1 min prior to fixation. hiCMs were fixed in the relaxed state in 4% PFA mixed in PBS supplemented with 1% Triton X-100 and 100uM s-nitro-blebbistatin for 45 min. Following fixation, cells were washed three times with PBS. When desired, cells were then incubated in either phalloidin488 or phalloidin568 (Thermo Fisher Scientific) for 2 h at 15:200μL dilution of phalloidin into PBS. Phalloidin was washed three times with PBS. Cells were blocked in 10% bovine serum albumin (BSA) in PBS for at least 20 min at room temperature, then primary antibodies were added in 10% BSA and incubated at 4C overnight. The next morning, cells were washed three times with 10% BSA, then cells were incubated in 10% BSA containing secondary antibodies for 1 h at room temperature. Cells were washed three times with PBS prior to imaging.

Human tissue stains

Tissue sections were from human myocardial tissue isolated from the left ventricular free wall. Formalin-fixed paraffin-embedded slides were first deparaffinized using Histoclear (National Diagnostics, HS-202) and then rehydrated through a series of decreasing ethanol concentrations in water. For antigen retrieval, slides were boiled for 1 h in a rice cooker with 10 mM Tris, 0.5 mM EGTA, pH 9 buffer. After cooling to room temperature, the slides were washed three times with phosphate-buffered saline (1X PBS). Tissue sections on the slides were delineated with a PAP pen, and then the slides were blocked for 1 h at room temperature with 10% normal goat serum (NGS; ab7481 Abcam). Primary antibodies were diluted in 1% NGS and incubated at 4°C overnight. The following day, slides were washed three times with 1X PBS, then incubated with secondary antibodies diluted in 1% NGS at room temperature in the dark. If needed, DRAQ5 was added during secondary antibody incubation to stain the nuclei. Afterward, slides were washed three times with 1X PBS, dehydrated using the reverse ethanol gradient, and mounted with Prolong Gold Antifade Mountant (P36930) with DAPI (P36931) if required, and sealed with clear nail polish.

Zebrafish stains

A modified version of the protocol from Inoue et al. was used for whole mount staining.[16] In detail, this modified protocol is described as follows: zebrafish embryos (72 h postfertilization) were first anesthetized in Tricaine on ice and then fixed overnight at 4°C in 4% PFA in PBS. The next day, the embryos were washed and gently rocked three times for 5–10 min each in PBT (PBS +0.1% Tween). Embryos were then incubated in 150 mM Tris-HCl (pH 9.0) for 5 min, heated at 70°C for 15 min, and subsequently washed twice in PBT for 5 min each, followed by two washes in deionized water for 5 min each. Next, the embryos were submerged in ice-cold pure acetone at −20°C for 20 min. After this, they were washed twice in deionized water for 5 min each and twice in PBT for 5 min each. Blocking was performed at room temperature for 3 h using a solution with 10% natural goat serum, 2% Triton X-100, and 1% BSA in PBT. After blocking, the embryos were incubated with primary antibodies in I-buffer (same as blocking solution but with 1% natural goat serum) at 4°C with gentle rocking for three days. Following primary antibody incubation, the embryos were washed three times for 1 h each in a solution of 10% goat serum and 2% Triton X-100 in 1X PBS, then twice for 1 h each in 2% Triton X-100 in 1X PBS. They were then incubated with secondary antibodies and DAPI at 4°C in the dark for 2.5 days. After incubation, the embryos were washed again three times for 1 h each in 10% goat serum and 2% Triton X-100 in 1X PBS, then twice for 1 h each in PBT. The primary antibody was used at a dilution of 1:100-1:200, the secondary antibody at 1:50, and DAPI was diluted to 100 μg/mL.

Antibodies used in this study

Alexa Fluor 647 goat anti-mouse IgG: Fisher Scientific A-21235.

MYH7: myosin heavy chain mouse IgG (DHSB: A4.951).

MYH6: atrium-specific myosin heavy chain (DHSB: S46).

Expression constructs

Constructs used in the study were purchased from Vectorbuilder as a bacterial stock.

mNeon-MYH7: contains the sequence for mNeon fused to the N-terminus of the consensus human *MYH7* sequence (NCBI reference sequence: NG_007884.1), separated by a 60bp linker.

mEGFP-MYH6: contains the sequence for mEGFP fused to the N-terminus of the consensus mouse *MYH6* sequence (NCBI reference: NC_000080.7), separated by a 60bp linker.

mEOS-MYH6: contains the sequence for mEOS fused to the N-terminus of the consensus human *MYH6* sequence (NCBI reference: NG_023444.1), separated by a 60bp linker.

Imaging

All images in the manuscript were acquired using a Nikon 100X immersion F-oil (refractive index 1.515) objective (NA = 1.45) of a Nikon CSU-W1 SoRa microscope in "SoRa mode" (i.e., at 240X), with the exception of zebrafish whole mount images, which were acquired using the Nikon 60X immersion F-oil objective (NA = 1.42). Images were deconvolved at 10 iterations using the Blind method prior to analyses. Exogenous expression of fusion proteins/co-labeling with secondary antibodies utilized mEGFP/mNeon in tandem with Alexa Fluor 647 to prevent bleed-through between channels. Integration times ranged from 100ms to 400ms.

QUANTIFICATION AND STATISTICAL ANALYSIS

All quantification was performed using the openly available analysis tool FIJI.[15] All statistical tests were performed using GraphPad Prism. For line scan averaging, in FIJI, a straight-line ROI of width 6 and length 2.6um was drawn with selection rotator toggled on. For each cell, the ROI was centered in the bare zone (i.e., at the M-line) of each sarcomere, rotated to be parallel with the filament long-axis, and saved to ROI manager. Once an ROI for each sarcomere had been saved to ROI manager, all ROIs were selected and fluorescence intensity was plotted using the multi-plot tool within FIJI's ROI manager "more" sub-menu. The fluorescence values were pasted into a Google Sheets document, compiled, and normalized using GraphPad Prism with maximum fluorescence value for each individual ROI set to 1. Following normalization, population averages were calculated from the average of all normalized fluorescence values for each biological replicate. The analysis was then re-performed using the MYH6 fluorescence channel using the same ROIs. Final plots generated represent average and standard error of the population means of each biological replicate. Cells were chosen for imaging based on expression level of the exogenously-introduced construct, with only dimmest cells analyzed to avoid overexpression artifacts.

To calculate distance extended from the filament center, the full length of each individually-measured filament in microns was first calculated from individual line scans as follows: fluorescence intensity for each line-scan was normalized to fluorescence maximum = 1 and filament length was calculated by measuring the length from half-max to half-max. Filament length was then divided by 2 and converted to nanometers. Statistical significance was defined as $p < 0.05$.